Single-electron tunneling through a double quantum dot: The artificial molecule

R. H. Blick, R. J. Haug, J. Weis, D. Pfannkuche, K. v. Klitzing, and K. Eberl
Max-Planck-Institut für Festkörperforschung, Heisenbergstrasse 1, 70569 Stuttgart, Germany
(Received 19 April 1995; revised manuscript received 16 November 1995)

Single-electron tunneling through two coupled quantum dots is strongly influenced by the electrostatic interaction between the dots. At low temperatures, we observe the formation of a molecularlike state in the double-dot system. The dots are defined by split gates in an $Al_xGa_{1-x}As$-GaAs heterostructure. They are of different size and coupled in series, leading to two different charging energies. In the linear transport regime we find the charging diagram for the double quantum dot. This diagram exhibits the operation points of the system to be employed as an electron pump.

Transport through zero-dimensional electron systems, so-called quantum dots, is dominated by Coulomb blockade effects and single-electron tunneling (SET).[1] Apart from these electrostatic phenomena, quantum effects become observable in nanoscale semiconductor devices.[2,3] The electronic properties of these single quantum dots have been experimentally investigated by transport or capacitance spectroscopy[2–5] and led to the expression ''artificial atom.''

Here, we study the conductance resonances of a double-dot system (DDS), consisting of two quantum dots of different size coupled in series by a tunneling barrier. In contrast to measurements on tunneling through a vertical double dot structure[6] our system is realized in a two-dimensional electron gas (2DEG) by a split-gate technique. The voltages of the gate electrodes determine the charging diagram of the DDS. From this diagram we extract the gate voltages at which our semiconductor DDS can be operated as a single-electron pump.[7] The charging diagram is strongly influenced by the interactions between the dots. There exist two interaction mechanisms: one is the electrostatic influence and the other is the direct coupling of electron wave functions in the different quantum dots. Concerning the electrostatic influence, a shift of the resonance condition for charging one dot occurs when another electron is added to the other dot. In these terms, one quantum dot acts as an electrometer measuring the charging process of the other dot, as is known from metallic systems[8] or from using a single split-gate channel as an electrometer.[9] Measurements performed by Ford *et al.*[10] show some features, which can be related to a two-dot system, while an electrostatic coupling was also found by Waugh *et al.*[11] In the case of direct coupling, an interaction of the wave functions is expected to form a molecularlike state, which can be imagined as a covalent binding of the two dots by an exchanged electron.[12] The Coulomb interaction is clearly seen in the measurements discussed below and indications for a coherent state within the DDS are also found.

The double quantum dots for lateral transport experiments are realized by patterning a 2DEG (90 nm below the substrate surface) with the help of split gates defined by electron-beam lithography in an $Al_xGa_{1-x}As$-GaAs heterostructure grown by molecular beam epitaxy. The carrier density at a temperature of 4.2 K is $n_s = 2.11 \times 10^{15}\ m^{-2}$ with a mobility of $\mu = 79\ m^2/Vs$. The geometry of the split gates is shown in the SEM micrograph in the left inset of Fig. 1. To define two quantum dots of different size, the following negative voltages are applied to the different gates: $V_{G4,5} = -335$ mV, $V_{G6,7} = -343$ mV, $V_{G1,2,3} = -767$ mV, and $V_{G9,10} = -1198$ mV. The separate definition of the two different quantum dots is also possible.[13]

The voltage of one side of the center split gate (V_{G8}) is varied in order to shift the electrostatic potentials of the quantum dots. In the description below, this center gate is called *top gate* (TG), since the other top-gate voltages are kept fixed. The opposite center gate is coupled deliberately to the lower left gate. A back gate (BG), situated 0.5 mm beneath the 2DEG, is used to additionally shift the electrostatic potentials of the quantum dots. The small and large quantum dots will be referred to as *A* and *B*, respectively. The con-

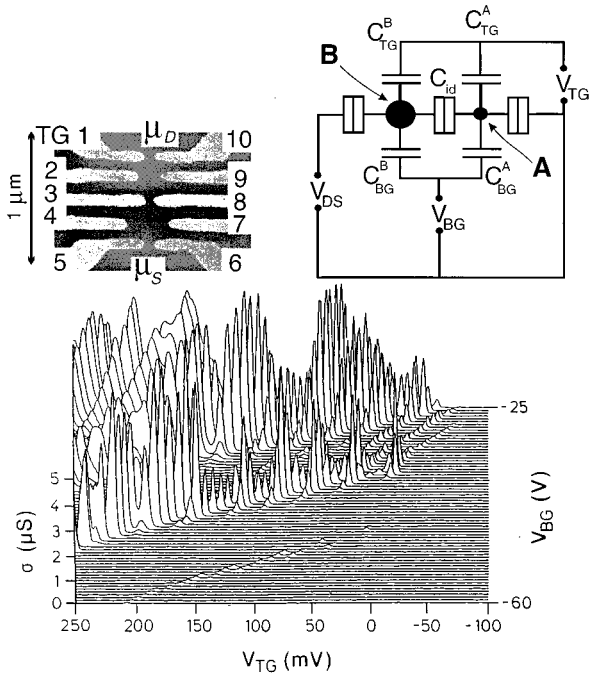

FIG. 1. Conductance σ of the double-dot system vs top-gate voltage V_{TG} for different back-gate voltages V_{BG} ranging from -60 V to -25 V. Left inset: SEM micrograph of the split-gate device. Right inset: simplified circuit diagram of the system.

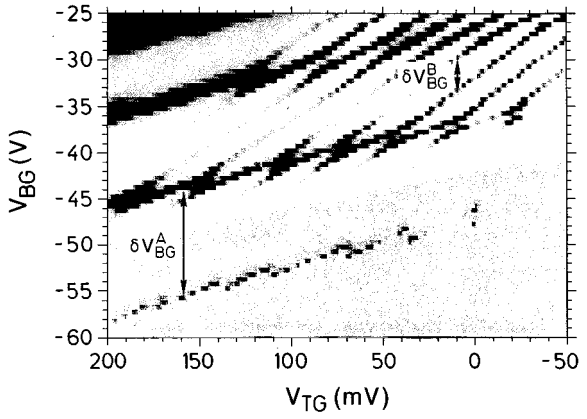

FIG. 2. The data of Fig. 1 shown as a gray-scale plot. The conductance data are represented in the range of $\sigma_{min}=0\ \mu$S (white) and $\sigma_{max}\geqslant 2\ \mu$S (black). In the lower part ($V_{BG}=-60$ V to ≈ -47 V) the conductance limits $\sigma_{min}=0\ \mu$S and $\sigma_{max}\geqslant 0.2\ \mu$S are chosen, to enhance the resolution.

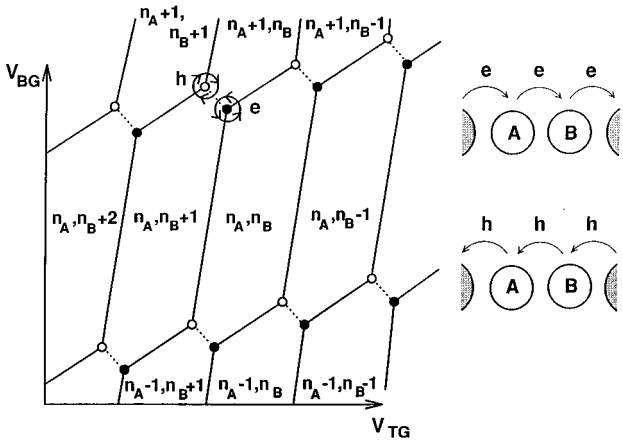

FIG. 3. A magnified part of the charging diagram in Fig. 2 is shown schematically. Different regions of Coulomb blockade (CB) are characterized by their charging state, e.g., (n_A,n_B) specifies the CB area with n_A electrons in dot A and n_B electrons in dot B. Full circles (●) denote the electron transfer process through the double-dot system sketched in the upper part of the inset, which corresponds to the counterclockwise path e. The empty circles (○) can be interpreted as the hole process (lower part of the inset), which corresponds to the clockwise path h.

ductivity measurements are performed in a ^{3}He/^{4}He dilution refrigerator with a base temperature of $T=23$ mK by using common lock-in amplification techniques with an excitation voltage of $V_{exc}=4.6\ \mu$V and a frequency of $\nu_{exc}=13$ Hz.

The conduction through these electron islands defined by the split gates is governed by the Coulomb blockade effect (CB). In Fig. 1 a plot of the conductance at zero drain-source voltage ($V_S=V_D$) as a function of the top-gate voltage (V_{TG}) is shown for different back-gate voltages (V_{BG}), stepping from $V_{BG}=-60$ V to -25 V with a step size of 0.5 V. Sharp conductance resonances representing single-electron tunneling are observed as a function of the gate voltages. A better representation of the DDS's conductance data is given in Fig. 2. Here the conductance is represented in a gray scale, where $\sigma_{min}=0\ \mu$S refers to white and $\sigma_{max}\geqslant 2\ \mu$S refers to black (upper part of Fig. 2). In the lower part of Fig. 2 the maximum conductance is set to $\sigma_{max}\geqslant 0.2\ \mu$S, to amplify the smaller conductance peaks. The important points to be noted are that in comparison to a single quantum dot, two gate voltages have to be varied to obtain a complete conductance resonance pattern. Passing a conductance resonance of either dot A or B will change the number of electrons in the DDS by one. This conductance resonance pattern can be interpreted as a charging diagram.

In contrast to the conductance resonances of a single quantum dot, the resonance pattern of the DDS shows *two* periodic oscillations, referring to the *two* charging or Coulomb blockade energies of two "single" dots. The energies are given by $E_C^A=e^2/C_\Sigma^A$ and $E_C^B=e^2/C_\Sigma^B$, where C_Σ^A, C_Σ^B represent the total capacitances of the dots A and B, respectively. The two kinds of resonances can be clearly distinguished in Fig. 2: one with a short period in gate voltage (δV_{BG}^B) and a large slope ($\delta V_{TG}^B/\delta V_{BG}^B$) and the other one with a long period (δV_{BG}^A) and a more gentle slope ($\delta V_{TG}^A/\delta V_{BG}^A$). The different periodicities of the two dots are marked in Fig. 2 and have values of $\delta V_{BG}^A\cong 13$V ($\delta V_{TG}^A\cong 220$ mV) for dot A and $\delta V_{BG}^B\cong 2.5$ V ($\delta V_{TG}^B\cong 22$ mV) for dot B. The period δV_{BG}^A of dot A varies, as is known to occur in very small quantum dots.[2] The different slopes result from the different capacitative couplings of the two dots to the top and back gates (see right inset of Fig. 1), which allows us to distinguish the different dots in the measurements. Using the drain source vs top-gate voltage dependence of these oscillations at $V_{BG}=-50$ V for calibration,[3] we find values for the Coulomb blockade energies of $E_C^A/2\cong 1.8$ meV and $E_C^B/2\cong 0.45$ meV. The total capacitances of the two dots are found to be $C_\Sigma^A=e^2/E_C^A\cong 45$ aF and $C_\Sigma^B=e^2/E_C^B\cong 178$ aF.

The appearance of two periodicities is readily comprehensible when considering two quantum dots connected in series. Without any electrostatic coupling a conductance resonance pattern will be found representing the superposition of the inverse of the conductivities,[14] $\sigma^{-1}=\sigma_A^{-1}+\sigma_B^{-1}$. Comparing the measured charging diagram of the DDS with the expected superposition of the resonance patterns of two separate dots, we observe a pronounced *"anticrossing"* of the resonance lines instead of a simple crossing. The "anticrossing" of the resonance lines indicates the electrostatic interaction between the two dots. The resonances in Fig. 2 can best be understood in the schematic charging diagram of Fig. 3. Depending on the two gate voltages (V_{TG} and V_{BG}) regions with different numbers of electrons n_A and n_B in dot A and B can be distinguished.[15] These regions are separated by boundaries which mark the change of the number of electrons in dot A and/or dot B by one electron. There are three different boundaries corresponding to the charging of dot A (α) or of dot B (β) with an electron from the leads (solid lines), and the exchange of an electron between both dots (γ, dotted line). These charging processes are possible when the following energy conditions in dependence of the gate voltages V_{BG} and V_{TG} are fulfilled: α, $E_{DD}^{el}(n_A+1,n_B)-E_{DD}^{el}(n_A,n_B)=eV_S$; β, $E_{DD}^{el}(n_A,n_B+1)-E_{DD}^{el}(n_A,n_B)=eV_D$; γ, $E_{DD}^{el}(n_A+1,n_B)-E_{DD}^{el}(n_A,n_B+1)=0$; where V_D and V_S give the electrostatic potentials of the drain and source lead. Using the notation of the circuit diagram (right

inset of Fig. 1) the electrostatic energy can be written as

$$E_{DD}^{el}=\frac{1}{2}Q_i\tilde{C}_{ij}Q_j+Q_i\tilde{T}_{ik}V_k, \tag{1}$$

regarding the Einstein sum convention with $i,j=A,B$, and k denoting all gate and lead contributions. The charges Q_A and Q_B are integer multiples of the electron charge, $Q_A=-n_Ae$ and $Q_B=-n_Be$. The inverted capacitance matrix $\tilde{C}_{ij}$ comprises the capacitance relations of the single dots and of the coupled system. The diagonal terms $\tilde{C}_{ii}\propto 1/C_\Sigma^i$ determine the charging energies of the isolated dots, while the off-diagonal elements $\tilde{C}_{ij}\propto C_{id}/(C_\Sigma^iC_\Sigma^j)$ with $i\neq j$ and $\tilde{C}_{AB}=\tilde{C}_{BA}$ are responsible for the ''anti-crossing.'' The values C_Σ^i $(i=A,B)$ are the total capacitances of the single dots which are found by the summation over the geometrical capacitances of the whole dot system. C_{id} denotes the interdot capacitance. The matrix $\tilde{T}_{ik}\propto[C_{ik}/C_\Sigma^i-C_{id}C_{jk}/(C_\Sigma^iC_\Sigma^j)]$ $(i\neq j)$ is dimensionless and describes the capacitative coupling of the dots A and B to the back gate, the top gates, and the leads.

For a DDS a conductance resonance is found when an electron is tunneling through *both dots*. The conditions for such a process are met, whenever three boundaries in the charging diagram (Fig. 3) meet in a point. *These triple points determine the gate voltages at which the DDS can be employed as a single-electron pump*.[7] We can distinguish two kinds of triple points, marked by a filled circle (●) and an open circle (○), which correspond to different transfer processes. The first process (●) is given by the following sequence of transitions: $(n_A,n_B)\rightarrow(n_A+1,n_B)\rightarrow(n_A,n_B+1)\rightarrow(n_A,n_B)$. This is marked by the counterclockwise path e in the charging diagram and is illustrated in the upper inset of Fig. 3 as an electron sequentially tunneling from one lead to the other. The energy conditions for these transitions are $E_{DD}^{el}(n_A,n_B)+eV_S=E_{DD}^{el}(n_A+1,n_B)=E_{DD}^{el}(n_A,n_B+1)$. The second process (○) is characterized by the sequence $(n_A+1,n_B+1)\rightarrow(n_A+1,n_B)\rightarrow(n_A,n_B+1)\rightarrow(n_A+1,n_B+1)$, marked by the clockwise path h. This can be interpreted as a sequential tunneling of a hole in a direction opposite to the electron, as is shown in the lower part of the inset of Fig. 3. In this case the energy conditions for the transitions are $E_{DD}^{el}(n_A+1,n_B+1)-eV_D=E_{DD}^{el}(n_A+1,n_B)=E_{DD}^{el}(n_A,n_B+1)$.[16] From the energy conditions for both processes (● and ○) it is found that the displacement (dashed line between e and h) of the two triple points is proportional to the interdot capacitance C_{id}. For electrostatically decoupled dots, i.e., $C_{id}\rightarrow 0$, the triple points are at the same position in the charging diagram. The electrostatic coupling lifts the degeneracy of these points and results in a splitting of the resonance conditions for different tunneling processes through the DDS.

In Fig. 2 the triple points are clearly seen together with the resonances marking the charging of dot A. The resonance corresponding to the charging of dot B is well pronounced in the upper right part of the measured charging diagram. The exchange of an electron between the dots (condition γ) occurs without a charge transfer from one lead to the other, thus, no conductance resonance is caused by this transition alone (dotted line in Fig. 3). Extending the resonance lines,

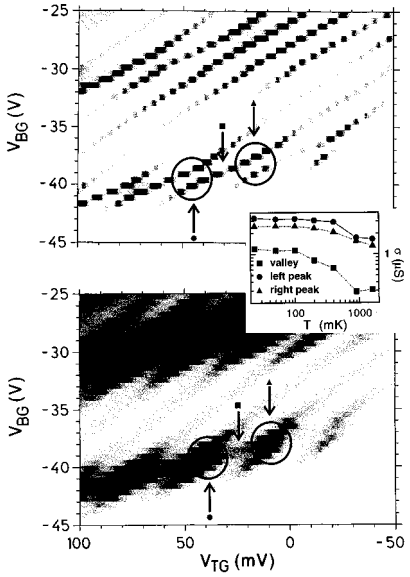

FIG. 4. Charging diagram of the double-dot system, taken at different temperatures $T=23$ mK (upper plot) and 1.6 K (lower plot). The gray-scale is given in the limits $\sigma_{min}=0$ μS (white) and $\sigma_{max}\geqslant 3$ μS (black). The arrows mark two triple points and the valley between them. In the inset the complete temperature dependence of the points marked by the arrows is given in a double-logarithmic representation.

the honeycomb pattern of Fig. 3 is found, formed by the Coulomb blockade regions. The splitting of the triple points caused by the electrostatic interdot coupling appears as an ''anticrossing'' of the resonance lines.

The mutual electrostatic influence can be identified by the steps found in the resonance lines which corresponds to a fixed charging process of one dot. This is best seen in the lowest resonance line of Fig. 2 around $V_{BG}=-55$ V, which represents the charging of dot A. At certain positions, steps occur resulting from the charging of dot B. *As dot B is charged with another electron, a sudden change in the electrostatic potential of dot A is induced, which shifts the resonance condition*. Thus, dot A acts as an electrometer measuring the charging processes of dot B. The step size is proportional to the strength of the electrostatic interdot coupling.

The observation of the conductance resonances away from the triple points contradicts the model of a strictly sequential tunneling process (see Fig. 2). The exchange of an electron between the dots without altering the total number of electrons in the system suggests the formation of a coherent mode in the DDS. Similar to the symmetric and antisymmetric wave functions in a double square-well potential[17] or the covalent binding in a molecule,[12] the electron in this mode cannot be localized in one of the dots. This coherent mode extends in the region between the splitted triple points (see points e and h in Fig. 3).

Since the temperature introduces a dephasing mechanism,[18] thus destroying a coherent mode, we determined the charging diagram as a function of the temperature. In Fig. 4 the diagram is shown at low and high temperatures ($T_l=23$ mK and $T_h=1.6$ K). The encircled regions mark some of the conductance peaks split due to the Coulomb

interaction between the dots. The positions marked by the arrows refer to two triple points and to the transition region between them, the so-called valley. In the inset of Fig. 4 the full temperature dependences of the valley of conductance and the two conductance triple points are given. As can be seen, the valley has a high conductivity at low temperatures, which saturates at temperatures below 100 mK, while at higher temperatures its conductance is considerably more suppressed than the triple points conductance. At $T=1.6$ K the decrease in conductance in the valley is almost 75% of the low temperature value. This behavior is also found for other valleys. Assuming sequential tunneling, conductance resonances are expected revealing a temperature-dependent broadening only, whereas the observed drastic *decrease* in conductance with *increasing* temperature indicates the existence of a coherent mode in the DDS. *This delocalized mode represents a molecular like state in the DDS*. At higher temperatures this state is dephased and only sequential tunneling is of importance. Thus, the molecularlike state decays into states localized at the two different ''artificial atoms.''

In summary, we presented transport measurements of a coupled DDS with two quantum dots of different size. The charging diagram of the DDS is determined by varying two gate voltages as external parameters. The triple points of this diagram are associated with the sequential tunneling of an electron, respectively of a hole through the DDS. They denote the voltages at which the device can be employed as a single-electron pump. The finite electrostatic coupling of the dots leads to an ''anticrossing'' of the conductance resonances. The existence of a coherent tunneling mode in the DDS is indicated by the fast decrease of conductance with increasing temperature.

We would especially like to thank V. Fal'ko for valuable and helpful discussions. We gratefully acknowledge discussions with H. Pothier, F. Stern, and K. Richter. We would like to thank Y. Kershaw for reading the manuscript. We acknowledge the technical support of A. Gollhardt, M. Riek, F. Schartner, and M. Schmidt. This work was funded by the Bundesministerium für Forschung und Technologie.

[1] For a review, see *Single Charge Tunneling-Coulomb Blockade Phenomena in Nanostructures, NATO Advanced Study Institute, Series B: Physics*, edited by H. Grabert and M.H. Devoret (Plenum Press, New York, 1992).

[2] P.L. McEuen *et al.*, Phys. Rev. Lett. **66**, 1926 (1991); R.C. Ashoori *et al.*, *ibid.* **71**, 613 (1993).

[3] J. Weis *et al.*, Phys. Rev. Lett. **71**, 4019 (1993).

[4] M. Tewordt *et al.*, Phys. Rev. B **46**, 3948 (1992).

[5] B. Su *et al.*, Phys. Rev. B **46**, 7644 (1992).

[6] U. Sivan *et al.*, Europhys. Lett. **25**, 605 (1994).

[7] H. Pothier *et al.*, Europhys. Lett. **17**, 249 (1992).

[8] P. Lafarge *et al.*, Z. Phys. B **85**, 327 (1991).

[9] M. Field *et al.*, Phys. Rev. Lett. **70**, 1311 (1993).

[10] C.J.B. Ford *et al.*, Nanostruct. Mater. **3** (1-6), 283 (1993).

[11] F.R. Waugh *et al.*, Phys. Rev. Lett. **75**, 705 (1995).

[12] W. Heitler and F. London, Z. Phys. **47**, 455 (1927).

[13] R.H. Blick *et al.* (unpublished).

[14] L.I. Glazman and V. Chandrasekhar, Europhys. Lett. **19**, 623 (1992); I.M. Ruzin *et al.*, Phys. Rev. B **45**, 13 469 (1993).

[15] Having this *charging diagram* defined, a regular conductance resonance pattern is obtained from which all resonance positions can be mapped. Varying only one gate voltage instead of two, the obtained conductance curve will show a stochasticlike distribution of resonance peaks at low temperatures. This is usually called ''stochastic Coulomb-blockade'' (Ref. 14). For a comparison with experimental data see M. Kemerink and L. Molenkamp, Appl. Phys. Lett. **65**, 1012 (1994).

[16] The triple points form the corners of the honeycomb lattice introduced by Pothier *et al.* (Ref. 7) for the metallic single-electron pump. In their case the triple points, corresponding to the electron and the hole process, respectively, are distinguished by the sign of the current.

[17] G. Baym, *Lectures on Quantum Mechanics* (Benjamin/Cummings Publishing Company, Inc., London, 1969).

[18] M. Büttiker, Phys. Rev. B **32**, 3020 (1986); P.W. Anderson *et al.*, Phys. Rev. Lett. **43**, 718 (1979).